Multiple Generations of Carbon in the Apex Chert and Implications for Preservation of Microfossils

Alison Olcott Marshall, Julienne R. Emry, and Craig P. Marshall

Abstract

While the Apex chert is one of the most well-studied Archean deposits on Earth, its formation history is still not fully understood. Here, we present Raman spectroscopic data collected on the carbonaceous material (CM) present within the matrix of the Apex chert. These data, collected within a paragenetic framework, reveal two different phases of CM deposited within separate phases of quartz matrix. These multiple generations of CM illustrate the difficulty of searching for signs of life in these rocks and, by extension, in other Archean sequences. Key Words: Apex chert—Carbonaceous material—Raman microspectroscopy—Paragenetic analysis—Archean. Astrobiology 12, 160–166.

1. Introduction

BILLIONS OF YEARS of plate tectonics have erased much of the Archean rock record and left the remaining rocks metamorphically altered and deformed, with typically poor exposures that make the rocks challenging to map and correlate. The Archean-aged rocks in the Pilbara Craton of Western Australia have been the subject of significant past research, as they have relatively good field exposure and are considered to have undergone low-grade metamorphic alteration at prehnite-pumpellyite (*ca.* 250–350°C) or lower greenschist facies (*ca.* 300–425°C) (Schopf, 1993; Blatt *et al.*, 2005; Brasier *et al.*, 2005; Van Kranendonk, 2006). These rocks also include the Apex chert, a carbon-containing unit (Brasier *et al.*, 2002, 2005; De Gregorio and Sharp, 2006; Marshall *et al.*, 2011) that has been proposed to contain the oldest putative microbial fossils on Earth (Schopf and Packer, 1987; Schopf, 1993). While the majority of studies have focused primarily on these structures (*e.g.*, Schopf and Packer, 1987; Brasier *et al.*, 2002; Schopf *et al.*, 2002; Marshall *et al.*, 2011), others have addressed the mode of formation and alteration of the Apex chert (*e.g.*, Van Kranendonk and Pirajno, 2004; Brasier *et al.*, 2005; Van Kranendonk, 2006).

This paper presents a Raman spectroscopic examination of the carbonaceous material (CM) present within the Apex chert in a paragenetic context, a combined approach that allows for the determination of the relative age of formation and thermal grade of the CM recently identified within the matrix of the Apex chert (Brasier *et al.*, 2002, 2005; De Gregorio and Sharp, 2006; Marshall *et al.*, 2011). Furthermore, these data suggest that the formation and alteration history of CM in other Archean rocks may be more complex than

previously thought and that an understanding of the degree of alteration of CM found within Archean deposits is critical when prospecting for evidence of the earliest life on Earth.

2. Geological Setting

The Pilbara Craton of Western Australia contains some of the oldest Archean rocks preserved on Earth (Fig. 1). An Archean proto-continent, the Pilbara Craton formed between 3.51 and 2.94 Ga as a volcanic plateau that consisted of a series of granitic complexes and volcanic rocks (Brasier *et al.*, 2005; Van Kranendonk, 2006). The Warrawoona Group, located in the East Pilbara Granite-Greenstone terrain in Western Australia, was formed between 3.42 and 3.15 Ga (Hickman, 1983; Brasier *et al.*, 2005). Its rocks consist of mafic extrusive volcanics and minor amounts of chert, barite, sulfides, carbonates, volcanoclastic units, and felsic volcanic horizons that have undergone prehnite-pumpellyite to greenschist facies metamorphism under low strain conditions (Brasier *et al.*, 2005; Van Kranendonk, 2006; Van Kranendonk *et al.*, 2007). Found within the Warrawoona Group, the Apex Basalt Formation consists primarily of komatiitic basalt with minor amounts of tholeiitic basalt, doleritic flows and dikes, and relatively thin (< 30 m) chert horizons (Brasier *et al.*, 2005). These mafic volcanic rocks show evidence of underwater eruption, including chilled margins, hyaloclastic breccias, and pillow basalt textures (Brasier *et al.*, 2005).

The Apex chert, which is geographically restricted to the Panorama Belt in the central part of the Pilbara Craton, is one of the thin chert horizons present in the Apex Basalt (Fig. 1). It consists of a series of black chert dikes and an overlying stratiform chert unit that occurs across three structural blocks
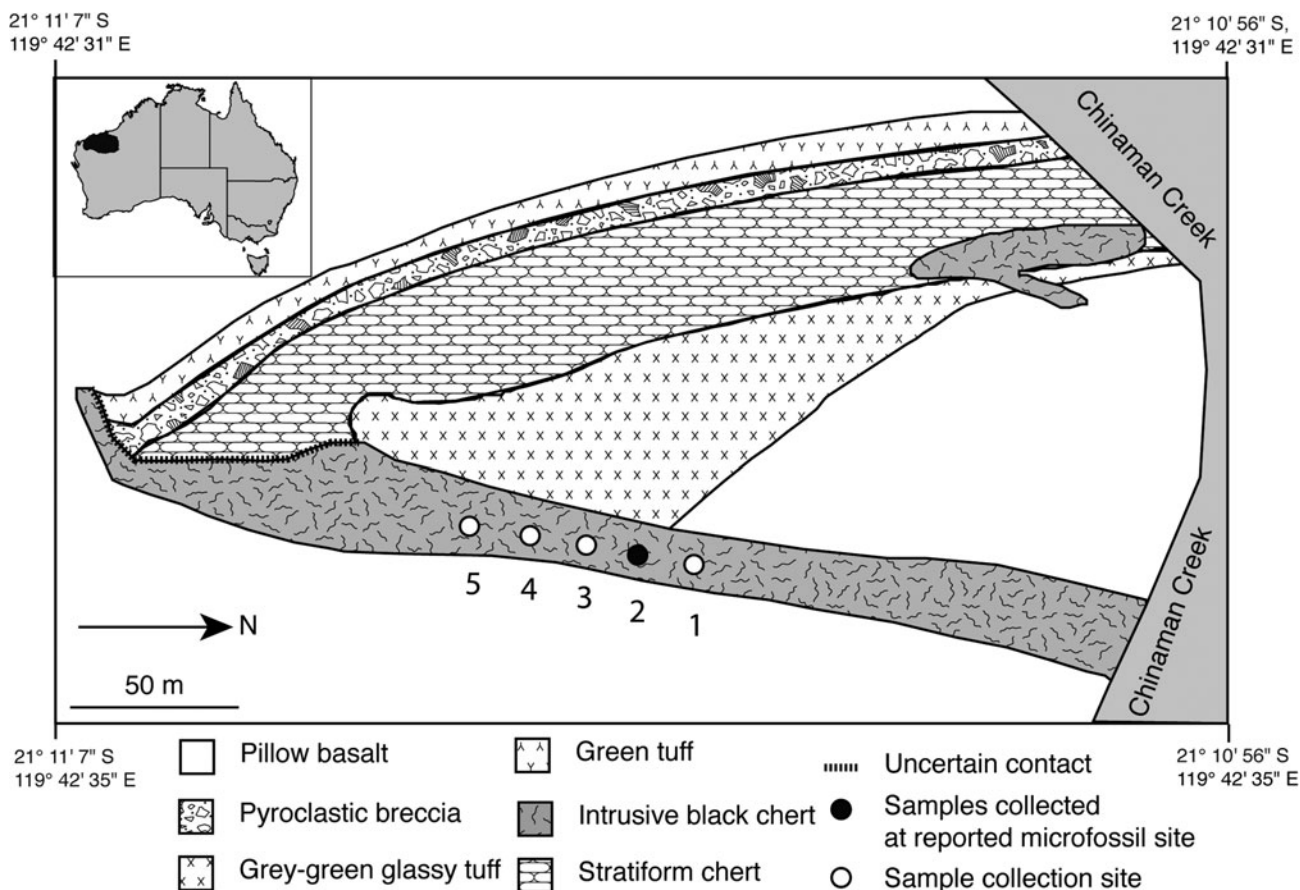
Department of Geology, University of Kansas, Lawrence, Kansas.

FIG. 1. Geological map of the Apex chert showing sample localities (modified from Brasier *et al.*, 2005). Circles represent sample collection sites; filled circle indicates original microfossil locality (Schopf and Packer, 1987). Inset map shows location of Pilbara Craton in Australia.

(North, South, and Central) that are defined by fault systems interpreted to be synsedimentary in origin (Fig. 1) (Brasier *et al.*, 2005). The dikes have been interpreted as feeder dikes that channeled hydrothermal fluids upward, which resulted in the formation of the overlying stratiform chert (Brasier *et al.*, 2005).

3. Materials and Methods

3.1. Sample collection

In 2006, samples were collected from the main Apex chert dike during the Geological Society of Western Australia Pilbara field trip (Fig. 1). The samples were collected approximately every 10 m up the outcrop, including at the original microfossil locality.

3.2. Microscopy

Petrographic analyses of the Apex chert were conducted on standard 30 μm thick petrological thin sections, which were made by Burnham Petrographic. Optical microscopy was performed on all thin sections with an Olympus BX51 System microscope.

3.3. Raman microspectroscopy

Standard point Raman spectra were collected with a Renishaw inVia Reflex Raman microprobe (Renishaw plc,

Wotton-under-Edge, UK), equipped with a Peltier cooled charge-coupled device (CCD) camera (1024×256 pixels). The spectrometer is fitted with holographic notch filters and five gratings [3600 mm/line (UV), 2400 mm/line (visible), 1800 mm/line (visible), 1200 mm/line (near IR), and 830 mm/line (near IR)]. The Raman light was dispersed by a diffraction grating with 2400 mm/line, and the signal was analyzed with a Peltier cooled CCD camera at room temperature (1024×256 pixels). The attached microscope is a Leica DMLM and is equipped with four objectives (×100/0.9 NA, ×50/0.75 NA, ×20/0.40 NA, ×5/0.12 NA) and a trinocular viewer that accommodates a video camera that allows direct viewing of the sample. Sample excitation was achieved with an argon ion laser (Modu-Laser, Utah, USA) emitting at 514.5 nm. Calibration of the Raman shift is achieved by recording the Raman spectrum of the silicon F_{1g} mode for one accumulation and 10 s. If necessary, an offset correction is performed to ensure that the position of the F_{1g} band is at $520.50 \pm 0.10 \, cm^{-1}$.

The laser power impinging on the CM was between 1 and 5 mW to minimize laser-induced heating of the samples (Marshall *et al.*, 2010). The Ar^+ laser was oriented normal to the sample. Graphite and other highly ordered sp^2 CM have strong structural anisotropy and thus do not exhibit the same Raman spectrum when the measurement is performed parallel or perpendicular to the *c* axis (*e.g.*, Katagiri *et al.*, 1988; Wang *et al.*, 1989; Compagnini *et al.*, 1997). The cherts studied here do not contain any foliation or penetrative fabric, and

the disordered sp^2 CM shows no preferred orientation. Therefore, in this case, it is possible that CM with different orientations in a single sample was analyzed. To examine this orientation effect, multiple measurements were obtained on each sample at different orientations. Repeated measurements for a single spot at different orientations show no spectral variation. It has been shown that polishing of thin sections and slabs can induce severe structural disorder in the CM lattice network and thus strongly influence the resulting Raman spectrum (*e.g.,* Nemanich and Solin, 1979; Pasteris, 1989; Mostefaoui *et al.,* 2000). In addition, when investigating Archean rocks, it is important to overrule surface contamination. Therefore, to avoid the two above-mentioned problems, the Raman measurements were made on CM particles of varying size embedded below the surface.

A refractive glass $100\times$ objective lens was used to focus the laser on a $1\,\mu m$ spot to collect the backscattered radiation. Collection parameters for the scans of the CM were $60\,s$ at $1–5\,mW$ with 100 accumulations over the full Raman region of $100–4000\,cm^{-1}$. The spectra were deconvoluted with a Gaussian/Lorentzian fit routine by using GRAMS/32 software to determine intensity of the D (I_D) and G (I_G) bands with accuracy. A mixed Gaussian/Lorentzian fit routine is used for disordered sp^2 CM (*e.g.,* Ferrari and Robertson, 2000; Takikawa *et al.,* 2001). The parameters were fitted to the experimental envelope by a least-squares iterative procedure. To determine the goodness of fit criteria, the following aspects were considered: (1) standard errors of parameters (χ-squared), (2) local poor fits (indicative of an incorrect choice of the number of component peaks or errors in their half-widths), and (3) the degree of coincidence of the second derivative (original and fitted spectrum). A total of 10 spectra were collected, and the standard deviation was calculated on the spread of the I_D/I_G ratios.

4. Application of Raman Microspectroscopy to Carbonaceous Material

Raman microspectroscopy provides molecular structural information on both inorganic and organic materials. While Raman spectroscopic data are collected over the full region of $100–4000\,cm^{-1}$, specific smaller regions are often examined for structural information of different materials. For instance, the mineral fingerprint region ($100–1800\,cm^{-1}$) is the portion of a Raman spectrum that contains diagnostic bands used to identify various minerals. The Raman spectrum of CM can be divided into first- and second-order regions, depending upon the degree of crystallinity of the CM. However, in the case of poor crystallinity there will be no bands in the second-order region. The carbon first-order region ($800–1800\,cm^{-1}$) is sensitive to the degree of two-dimensional ordering present in CM, while the carbon second-order region ($2200–3400\,cm^{-1}$) is sensitive to the three-dimensional ordering of the CM and indicates the degree of its graphitization (Lespade *et al.,* 1982). The carbon first-order region generally contains two broad bands from CM; the first, commonly referred to as the D band, is seen at $\sim 1350\,cm^{-1}$ and is assigned to an A_{1g} symmetry mode that becomes Raman active with disorder. The second, referred to as the G band, is seen at $\sim 1600\,cm^{-1}$ and is assigned to the E_{2g2} symmetry mode. The carbon second-order region shows several bands at 2450, 2695, 2735, 2950, and $3248\,cm^{-1}$, all of which are assigned to both overtone and combination scattering. The ratio of the intensity of the D and G bands (I_D/I_G) has been shown to reflect the degree of structural order and thermal evolution in CM (*e.g.,* Jehlicka and Bény, 1992; Jehlicka *et al.,* 2003), and graphing the intensity of the D/G (I_D/I_G) bands of each sample against the area of the D/G (A_D/A_G) bands can reveal differences between the thermal evolution or metamorphic grades of CM (*e.g.,* Pasteris and Wopenka, 1991; Jehlicka and Bény, 1992; Wopenka and Pasteris, 1993; Yui *et al.,* 1996; Jehlicka *et al.,* 2003; Tice *et al.,* 2004). It should be noted that, in these studies of the thermal evolution of natural CM, either a $514.5\,nm$ ($2.41\,eV$) or a $532\,nm$ ($2.33\,eV$) laser was used. Over the $244–1064\,nm$ range of laser excitation, the G band position and intensity are practically independent of excitation wavelength, whereas the D band shows an apparent linear variation of its position (amounting to about $180\,cm^{-1}$ in the measured range), and its intensity (Pocsik *et al.,* 1998) strongly depends on the excitation wavelength. This phenomenon is attributed to a resonance enhancement effect of the D band (Pocsik *et al.,* 1998). Recently, Aoya *et al.* (2010) showed that there is little to no difference in I_D/I_G and A_D/A_G ratios for the same CM sample acquired from either excitation with a 514.5 or $532\,nm$ laser. Therefore, it is valid to undertake a comparison of the above I_D/I_G ratios from the literature to delineate the thermal evolution of CM collected with either a 514.5 or $532\,nm$ laser.

Carbonaceous material contains crystallites of the order of nanometers in diameter, which are composed of graphite-like layers of aromatic clusters that are arranged turbostratically (*i.e.,* layers randomly stacked perpendicular to the crystallographic *c* axis). Tuinstra and Koenig (1970a, 1970b) clearly demonstrated a relationship between the intensity ratio of the D and G bands (commonly denoted as I_D/I_G) and the microcrystalline planar size L_a. Calibration against the in-plane crystallite size (L_a), as measured by X-ray diffraction, has shown that the ratio of Raman intensities of the D and G bands is inversely proportional to the average value of L_a. Knight and White (1989) measured the Raman spectra of numerous sp^2 CM, using an excitation wavelength of $514.5\,nm$ ($E_1 = 2.41\,eV$), and derived an empirical expression that allows the determination of L_a from the intensity ratio of D and G bands given by: $L_a = 44[I_D/I_G]^{-1}$ (nm). Later on, Mernagh *et al.* (1984) showed that the I_D/I_G ratio depends strongly on the excitation laser energy (E_1) used in the Raman analysis, which thus revealed that the Knight and White (1989) empirical formula was only valid when the analysis was performed with the $514.5\,nm$ laser line. It has been shown that this relationship holds for a wide range of sp^2-bonded carbons over the range of $2.5 < L_a < 300\,nm$.

5. Results

5.1. Raman microspectroscopy of carbonaceous material from the Apex chert

Raman microspectroscopy revealed two different phases of CM present within all samples from the Apex chert (Fig. 2). Within the mineral fingerprint region ($100-1800\,cm^{-1}$), both phases contain bands at 206, 464, and $511\,cm^{-1}$, all of which can be assigned to vibrational modes (A_1 symmetry) of quartz. While both phases of CM contain D ($\sim 1350\,cm^{-1}$) and G ($\sim 1600\,cm^{-1}$) bands, the line-shapes of the bands are markedly different for each phase of CM. In one phase, the D and G bands are of similar intensity and are relatively broad.
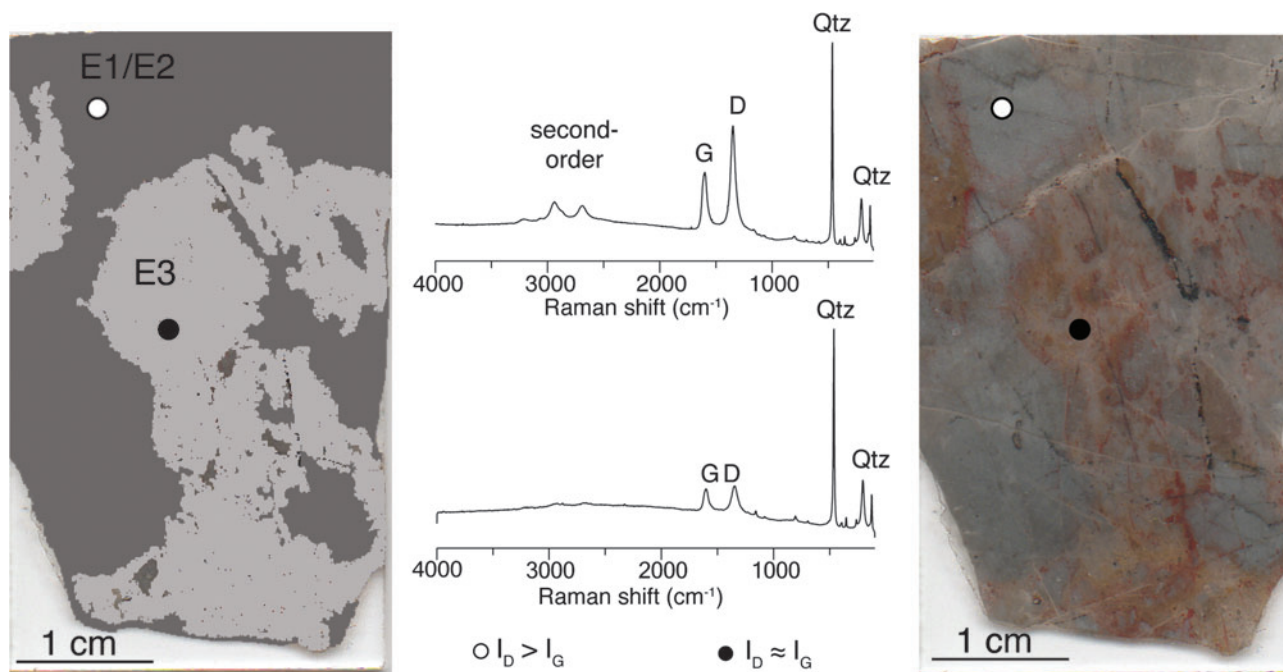
FIG. 2. Raman spectra of CM within its paragenetic framework. Thin section on right, collected at the original microfossil locality, reveals the complex alteration history of the Apex chert, most noticeably the multiple generations of matrix formation. The sketch on the left illustrates the relationship between the first two phases of the matrix formation (E1/E2) and the third phase (E3). The top Raman spectrum was collected within the E1 matrix (the white dot), while the bottom one was collected within the E3 matrix (the black dot). The carbon first-order bands are denoted "D" and "G," the carbon second-order bands are denoted "second-order," and the quartz bands are denoted "Qtz."

In contrast, the other phase has a D band that is more intense than the G band and most notably contains additional bands in the carbon second-order region at 2695 and 2950 cm^{-1}.

The CM with D and G bands of similar intensity found within all the Apex chert samples has an I_D/I_G ratio of 1.27 ± 0.12, while the phase with a more intense D band has a ratio of 1.68 ± 0.15. The microcrystalline planar size L_a also varies for each CM phase from 35 to 26 nm based on the Knight and White (1989) calibration. Comparison of the intensity of the D band, I_D/I_G ratio (Fig. 3), presence and absence of second-order bands, and L_a revealed that these comprise two different populations of CM.

5.2. Petrographic analysis of the Apex chert

Paragenetic analyses allowed for determination of a detailed geological history by examining mineral phases and assemblages on a microscopic scale. Furthermore, this technique can provide an understanding of the timing and thermal history of the two phases of CM identified by Raman spectroscopy. It has been interpreted that the Apex chert is a brecciated hydrothermal chert related to granitoid intrusions with multiple pulses of hydrothermal silica during formation (Brasier *et al.*, 2002, 2005; Van Kranendonk and Pirajno, 2004; Van Kranendonk 2006). Our petrographic analysis showed that the formation of the quartz matrix can be broken into four major phases, which may suggest four major pulses of repeated hydrothermal silica injection during vein formation.

The first phase of matrix formation (E1) was the deposition of clasts of gray microcrystalline quartz that contained small black particles of CM. Raman microspectroscopy of the

CM preserved in E1 revealed the phase with a more intense D band (Fig. 2), I_D/I_G ratio of 1.68 ± 0.15 (Fig. 3), a L_a of 26 nm, and the presence of well-developed second-order bands. Clasts of E1 are contained within a clear to light gray microcrystalline quartz matrix (E2) (Fig. 2). E1 and E2 record deposition of a clastic rock that was then entombed in microcrystalline quartz matrix. The second major phase (E3) of
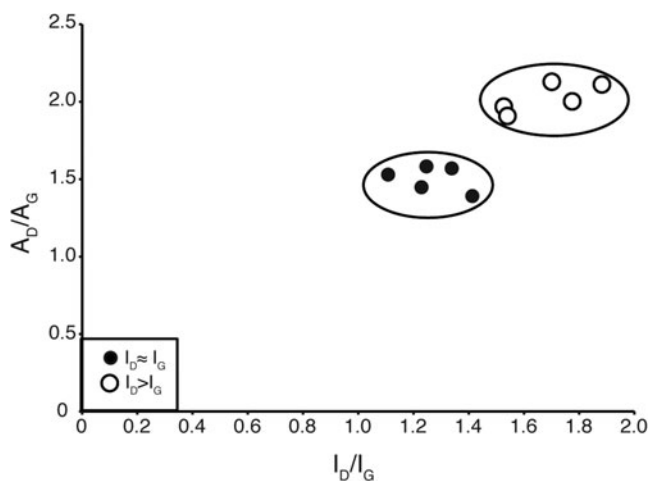

FIG. 3. Graph comparing the intensity (I_D/I_G) and the area (A_D/A_G) ratios of the CM. This comparison reveals the presence of two populations of CM, one in which the D band is roughly equal to the G band (filled circles) and one in which the D band is larger than the G band (open circles).

matrix formation consists of light gray or gray-pink micro-crystalline quartz that contains light-gray to brown clots of CM, small dark brown-black particles of CM and sub-microscopic disseminated CM (Fig. 2). Raman microspectro-scopy of this CM revealed that it is all composed of the phase of CM in which the D and G bands are of similar intensity (Fig. 2), I_D/I_G ratio of 1.27 ± 0.12 (Fig. 3), a L_a of 35 nm, and the absence of notable second-order bands. It is apparent that the E3 phase occurred after the formation of the clasts and matrix in E1 and E2, as pieces of the E1-E2 phase are present within the quartz matrix of the E3 phase. The relationships of the E1-E3 phases are illustrated in the sketch in Fig. 2. The final phase (E4) of the matrix formation consists of clear, micro-macrocrystalline quartz that does not contain CM and occurs as irregular patches and thin veins.

6. Discussion

Several researchers have shown that the degree of disorder in natural CM is related to the degree of thermal evolution and metamorphism, which in turn produces characteristic carbon first-order Raman spectra line-shapes (e.g., Pasteris and Wopenka, 1991; Jehlicka and Bény, 1992; Wopenka and Pasteris, 1993; Marshall et al., 2001; Jehlicka et al., 2003). Furthermore, as CM does not undergo retrograde metamor-phism, it is a useful proxy for the peak metamorphic grade or thermal alteration experienced by the host rock (e.g., Pasteris and Wopenka, 1991; Jehlicka and Bény, 1992; Wopenka and Pasteris, 1993; Marshall et al., 2001; Beyssac et al., 2002; Jehlicka et al., 2003; Aoya et al., 2010). Thus, comparison of the line-shape and spectral parameters (i.e., I_D/I_G ratio) of the Raman spectra of CM found within the Apex chert to that of CM from deposits of known metamorphic grade and thermal evolution allows for a semiquantitative elucidation of the thermal al-teration history of the CM (but it does not allow for deter-mination of an absolute temperature value). As the Raman spectra were collected within a paragenetic framework, it is also possible to gain an understanding of the relative timing of the deposition of the CM.

The CM found in phase E3 has a line-shape similar to carbon first-order Raman spectra from CM found in several deposits metamorphosed to lower greenschist facies, in-cluding Neoproterozoic units in the Bohemian Massif (Jeh-licka et al., 2003) and Paleoproterozoic cherts from Shunga, Russia (Wopenka and Pasteris, 1993). In contrast, the CM found in phase E1 has a line-shape similar to carbon first-order Raman spectra from CM found in thermally more mature deposits. These include CM from Neoproterozoic units in the Bohemian Massif that experienced amphibolite facies metamorphism (ca. 500–700°C) (Jehlicka et al., 2003; Blatt et al., 2005), as well as upper greenschist facies (ca. 425–500°C) Archean deposits from the Swaziland sequence (Pasteris and Wopenka, 2003) and the Barberton greenstone belt (Tice et al., 2004; Van Zuilen et al., 2007).

These differences, as well as the fact that the CM found in the E1 phase also resolved bands in the carbon second-order region, indicate that this phase of CM has more three-dimensional ordering and thus represents a higher thermal alteration. Furthermore, Marshall et al. (2001, 2007), and Lahfid et al. (2010) demonstrated that Raman spectra ac-quired from CM thermally altered from 230°C to 300°C shows that the relative intensity of the D band progressively increases. Between temperatures of 300–350°C, the D band intensity is higher than the G band intensity (Marshall et al., 2001, 2007; Lahfid et al., 2010). Additionally, there are several indicators that the CM in phase E1 must have been deposited before the less thermally mature CM in phase E3. First, the distribution of the CM within two different phases of matrix indicates that it was deposited at different times, and E3 contains a younger phase of CM than E1. Second, CM does not undergo retrograde thermal alteration or metamorphism, but instead records peak thermal stress; thus, the more thermally altered CM must have been heated before the less altered CM was deposited. Third, the fact that the CM in the E1 phase records thermal alteration to temperatures equiv-alent of upper greenschist or perhaps even amphibolite facies suggests several possible scenarios for the deposition and preservation of the CM. First, these observed temperatures could be due to the Apex chert experiencing a higher degree of metamorphic alteration than previously suspected. Alter-natively, the CM could be allochthonous and represent a phase of transported thermally altered CM that is younger than the chert. Finally, the thermal alteration could have occurred if CM was emplaced multiple times by pulses of hydrothermal silica of varying temperature. While the data do not allow discrimination between these scenarios, none support a biogenic origin for the CM.

6.1. Implications for the search for ancient life in Archean sequences

The presence of two phases of CM within these samples complicates the search for ancient life in the Apex chert and, by extension, in other Archean sequences. The presence of two separate generations of CM indicates that not all the carbon, if any, found within the samples is primary, as CM was deposited after the initial formation of the rock unit. Thus, it is not possible to determine whether the CM ana-lyzed is syngenetic. As paired Raman spectroscopic and paragenetic analyses have not been performed on other Ar-chean sequences, it is not possible to know whether other rocks have a similar distribution of CM. However, re-searchers have applied Raman microspectroscopy to multi-ple particles of CM within single Archean samples, and these data are suggestive of the fact that other Archean sequences might also harbor multiple populations of CM. For instance, analyses of CM particles found within single samples of the 3.5–3.2 Ga Onverwacht and Fig Tree Groups of the Barberton greenstone belt in South Africa produced I_D/I_G measure-ments with a standard deviation of 15% (Tice et al., 2004). This value is much larger than the 9% standard deviations seen in each CM population in the Apex chert and is in fact similar to the 17% standard deviation obtained if the sepa-rate populations are considered as one (average $I_D/I_G = 1.48 \pm 0.25$). Similarly, Raman microspectroscopy on multiple carbonaceous particles from the Pilbara Craton that are of similar age to the Apex chert but were collected ca. 50 km west were found to have I_D/I_G measurements that ranged from 1.0 to 1.6 (Ueno et al., 2001), a very similar range to what was observed across the two populations of CM in the Apex chert (1.27–1.68). While the only spectra pictured show the D band to be larger than the G band, which is similar to what was exhibited by the CM found in the E1 matrix, an I_D/I_G measurement of 1 indicates that the D band is of equal

intensity to the G band, which is similar to what was exhibited by the CM found in the E3 matrix. Sugitani *et al.* (2010) showed that Raman spectra collected on carbonaceous microstructures from the 3.4 Ga Strelley Pool Formation had I_D/I_G ratios varying between 1.25 and 1.94.

Micrometer-scale heterogeneities in CM may be explained by a variety of mechanisms, such as micrometer-scale differences in precursor chemistry of CM, and subsequently dissimilar alteration pathways of the different precursor material, allochthonous CM, or emplacement of CM during multiple hydrothermal pulses at different temperatures. The possibility that Archean rocks contain multiple generations of CM also has ramifications for any potential carbonaceous microstructures that are found within the rocks. If CM has been deposited in different episodes of matrix formation and essentially acts as a reworked sedimentary particle, it is also then possible that a carbonaceous microstructure could have been deposited sometime after the initial formation of the rock. Thus, these data reveal that when searching for microfossils, it is of paramount importance to consider the paragenetic context of the carbonaceous microstructures and not to rely on context-free kerogen isolates or paleontological thin sections (*ca.* 300 μm) that obscure the petrological details of the matrix fabric (Marshall *et al.*, 2011).

7. Conclusion

The Raman spectroscopic analyses of the CM found within the Apex chert revealed the presence of two generations of CM with two different thermal alteration histories. Paragenetic analyses also revealed that these two populations of CM are found within two different episodes of matrix formation. Taken together, these data indicate that there are several generations of CM contained within the Apex chert, none of which might be syngenetic with the initial formation of the sequence. Although other Archean sequences have not yet been analyzed with this combination of techniques, Raman microspectroscopy analysis of the CM found in other Archean deposits has been suggestive of the idea that they, too, might contain multiple generations of CM. The possibility that CM is being redeposited within these rocks illustrates the need for caution when searching for carbonaceous microfossils, as well as the importance of conducting this search within a paragenetic framework.

Acknowledgments

Abbreviation

CM, carbonaceous material.

References

Aoya, M., Kouketsu, M., Endo, S., Shimizu, H., Mizukami, T., Nakamura, D., and Wallis, S. (2010) Extending the applicability of the Raman carbonaceous material geothermometer using data from contact metamorphic rocks. *Journal of Metamorphic Geology* 28:895–914.

Beyssac, O., Goffé, B., Chopin, C., and Rouzard, J.N. (2002) Raman spectra of carbonaceous material in metasediments: a new geothermometer. *Journal of Metamorphic Geology* 20:859–871.

Blatt, H., Tracy, R., and Owens, B. (2005) *Petrology: Igneous, Sedimentary, and Metamorphic*, 3rd ed., W.H. Freeman and Company, New York.

Brasier, M.D., Green, O.R., Jephcoat, A.P., Kleppe, A.K., Van Kranendonk, M.J., Lindsay, J.F., Steele, A., and Grassineau, N.V. (2002) Questioning the evidence for Earth's oldest fossils. *Nature* 416:76–81.

Brasier, M.D., Green, O.R., Lindsay, J.F., McLoughlin, N., Steele, A., and Stoakes, C. (2005) Critical testing of Earth's oldest putative fossil assemblage from the ~3.5 Ga Apex chert, Chinaman Creek, Western Australia. *Precambrian Res* 140:55–102.

Compagnini, G., Puglist, O., and Foti, G. (1997) Raman spectra of virgin and damaged graphite edge planes. *Carbon* 35:1793–1797.

De Gregorio, B.T. and Sharp, T.G. (2006) The structure and distribution of carbon in 3.5 Ga Apex chert: implications for the biogenicity of Earth's oldest putative microfossils. *Am Mineral* 91:784–790.

Ferrari, A.C. and Robertson, C. (2000) Interpretation of Raman spectra of disordered and amorphous carbon. *Phys Rev B Condens Matter Mater Phys* 61:14095–14107.

Hickman, A.H. (1983) Geology of the Pilbara Block and its environs. *Bulletin of the Geological Survey of Western Australia* 127:1–267.

Jehlicka, J. and Bény, C. (1992) Application of Raman microspectrometry in the study of structural changes in Precambrian kerogens during regional metamorphism. *Org Geochem* 18:211–213.

Jehlicka, J., Urban, O., and Pokorný, J. (2003) Raman spectroscopy of carbon and solid bitumens in sedimentary and metamorphic rocks. *Spectrochim Acta A Mol Biomol Spectrosc* 59:2341–2352.

Katagiri, G., Ishida, H., and Ishitani, A. (1988) Raman spectra of graphite edge plane. *Carbon* 26:565–571.

Knight, D.S. and White, W.B. (1989) Characterization of diamond films by Raman spectroscopy. *J Mater Res* 4:385–393.

Lahfid, A., Beyssac, O., Deville, E., Negro, F., Chopin, C., and Goffe, B. (2010) Evolution of the Raman spectrum of carbonaceous material in low-grade metasediments of the Glarus Alps (Switzerland). *Terra Nova* 22:354–360.

Lespade, P., Al-Jishi, R., and Dresselhaus, M.S. (1982) Model for Raman scattering from incompletely graphitized carbons. *Carbon* 20:427–431.

Marshall, C.P., Mar, G.L., Nicoll, R.S., and Wilson, M.A. (2001) Organic geochemistry of artificially matured conodonts. *Org Geochem* 32:1055–1071.

Marshall, C.P., Love, G.D., Snape, C.E., Hill, A.C., Allwood, A.C., Walter, M.R., Van Kranendonk, M.J., Bowden, S.A., Sylva, S.P., and Summons, R.E. (2007) Structural characterization of kerogen in 3.4 Ga Archaean cherts from the Pilbara Craton, Western Australia. *Precambrian Res* 155:1–23.

Marshall, C.P., Edwards, H.G.M., and Jehlicka, J. (2010) Understanding the application of Raman spectroscopy to the detection of traces of life. *Astrobiology* 10:229–243.

Marshall, C.P., Emry, J.R., and Olcott Marshall, A. (2011) Haematite pseudomicrofossils present in the 3.5-billion-year-old Apex chert. *Nat Geosci* 4:240–243.

Mernagh, T.P., Cooney, R.P., and Johnson, R.A. (1984) Raman spectra of graphon carbon black. *Carbon* 22:39–42.

Mostefaoui, S., Perron, C., Zinner, E., and Sagon, G. (2000) Metal associated carbon in primitive chondrites: structure, isotopic composition and origin. *Geochim Cosmochim Acta* 64:1945–1964.

Nemanich, R.J. and Solin, S.A. (1979) First- and second-order Raman scattering from finite-size crystals of graphite. *Physical Review B* 20:392–401.

Pasteris, J.D. (1989) *In situ* analysis in geological thin-sections by laser Raman microprobe microspectroscopy: a cautionary note. *Appl Spectrosc* 43:567–570.

Pasteris, J.D. and Wopenka, B. (1991) Raman spectra of graphite as indicators of degree of metamorphism. *Canadian Mineralogist* 29:143–153.

Pasteris, J.D. and Wopenka, B. (2003) Necessary, but not sufficient: Raman identification of disordered carbon as a signature of ancient life. *Astrobiology* 3:727–738.

Pocsik, I., Hundhausen, M., Koos, M., and Ley, L. (1998) Origin of the D peak in the Raman spectrum of microcrystalline graphite. *J Non Cryst Solids* 227–230:1083–1086.

Schopf, J.W. (1993) Microfossils of the Early Archean Apex Chert: new evidence of the antiquity of life. *Science* 260:640–646.

Schopf, J.W. and Packer, B.M. (1987) Early Archean (3.3-billion to 3.5-billion-year-old) microfossils from Warrawoona Group, Australia. *Science* 237:70–73.

Schopf, J.W., Kudryavtsev, A.B., Agresti, D.G., Wdowiak, T.J., and Czaja, A.D. (2002) Laser-Raman imagery of Earth's earliest fossils. *Nature* 416:73–76.

Sugitani, K., Lepot, K., Nagaoka, T., Mimura, K., Van Kranendonk, M., Oehler, D.Z., and Walter, M.R. (2010) Biogenicity of morphologically diverse carbonaceous microstructures from the *ca.* 3400 Ma Strelley Pool Formation, in the Pilbara Craton, Western Australia. *Astrobiology* 10:899–920.

Takikawa, H., Tao, Y., Miyano, R., Sakakibara, T., Ando, Y., Zhao, X., Hirahara, K., and Iijima, S. (2001) Carbon nanotubes on electrodes in short-time heteroelectrode arc. *Mater Sci Eng C Mater Biol Appl* 16:11–16.

Tice, M.M., Bostick, B.C., and Lowe, D.R. (2004) Thermal history of the 3.5–3.2 Ga Onverwacht and Fig Tree Groups, Barberton greenstone belt, South Africa, inferred by Raman microspectroscopy of CM. *Geology* 32:37–40.

Tuinstra, F. and Koenig, J.L. (1970a) Raman spectrum of graphite. *J Chem Phys* 53:1126–1130.

Tuinstra, F. and Koenig, J.L. (1970b) Characterization of graphite fiber surfaces with Raman spectroscopy. *J Compos Mater* 4:492–499.

Ueno, Y., Isozaki, Y., Yurimoto, H., and Maruyama, S. (2001) Carbon isotopic signatures of individual Archean microfossils(?) from Western Australia. *Int Geol Rev* 43:196–212.

Van Kranendonk, M.J. (2006) Volcanic degassing, hydrothermal circulation and the flourishing of early life on Earth: a review of the evidence from *c.* 3490–3240 Ma rocks of the Pilbara Supergroup, Pilbara Craton, Western Australia. *Earth-Science Reviews* 74:197–240.

Van Kranendonk, M.J. and Pirajno, F. (2004) Geological setting and geochemistry of metabasalts and alteration zones associated with hydrothermal chert±barite deposits in the *ca.* 3.45 Ga Warrawoona Group, Pilbara Craton, Australia. *Geochemistry: Exploration, Environment, Analysis* 4:253–278.

Van Kranendonk, M.J., Smithies, R.H., Hickman, A.H., and Champion, D.C. (2007) Review: secular tectonic evolution of Archean continental crust: interplay between horizontal and vertical processes in the formation of the Pilbara Craton, Australia. *Terra Nova* 19:1–38.

Van Zuilen, M.A., Chaussidon M., Rollion-Bard, C., and Marty, B. (2007) Carbonaceous cherts of the Barberton greenstone belt, South Africa: isotopic, chemical and structural characteristics of individual microstructures. *Geochim Cosmochim Acta* 71:655–669.

Wang, A., Dhamelincourt, P., Dubessy, J., Guerard, D., Landais, P., and Lelaurain, M. (1989) Characterization of graphite alteration in an uranium deposit by micro-Raman spectroscopy, X-ray diffraction, transmission electron microscopy and scanning electron microscopy. *Carbon* 27:209–218.

Wopenka, B. and Pasteris, J.D. (1993) Structural characterization of kerogens to granulite-facies graphite; applicability of Raman microprobe spectroscopy. *Am Mineral* 78:533–557.

Yui, T.-F., Huang, E., and Xu, J. (1996) Raman spectrum of carbonaceous material: a possible metamorphic grade indicator for low-grade metamorphic rocks. *Journal of Metamorphic Geology* 14:115–124.

Address correspondence to:
Craig P. Marshall
Department of Geology
University of Kansas
Lawrence, KS 66045

E-mail: cpmarshall@ku.edu